SUPPORTING INFORMATION

Forward and Backward Extinction Measurements on a Single Supported Nanoparticle: Implications of the Generalized Optical Theorem

Michel Pellarin, Christophe Bonnet, Jean Lermé, Floriane Perrier, Julien Laverdant, Marie-Ange Lebeault, Sylvain Hermelin, Matthias Hillenkamp, Michel Broyer, and Emmanuel Cottancin

Université de Lyon, Université Claude Bernard Lyon 1, CNRS, Institut Lumière Matière, F-69622, VILLEURBANNE, France

1. Supported gold nanocubes

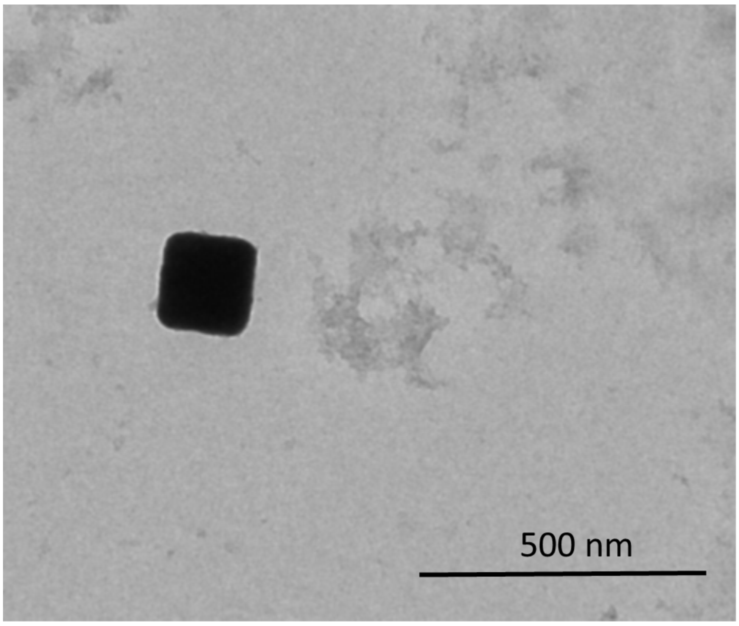

Figure S1: Transmission electron microscopy image of a 160 nm gold nanocube supported on a Formvar resin film.

2. <u>Reproducibility of SMS measurements on single nanocubes</u>

Spatial modulation spectroscopy measurements have been performed on several gold nanocubes deposited on a Formvar resin film or glass microscope coverslip. They are displayed in Figure S2 and S3 below.

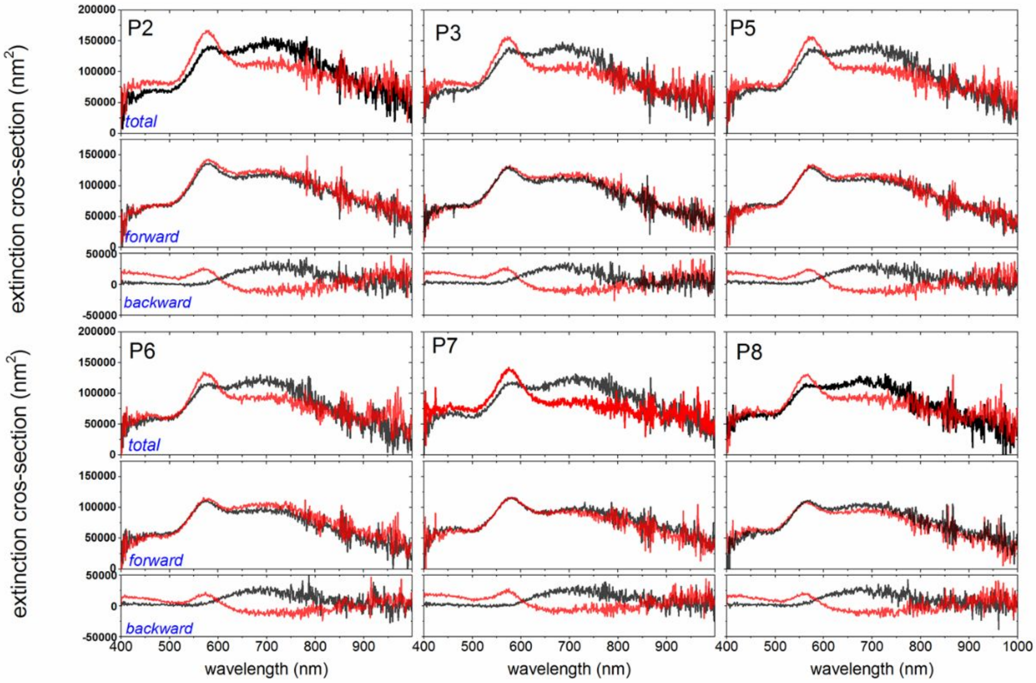

.

<u>Figure S2</u>: Corrected extinction cross-sections in the backward and forward directions, as well as their sum (total), measured for various 160 nm gold nanocubes supported on a thin Formvar film (red curves: particle in front of the film (UP position), black curves: particle behind the film (DOWN position)).

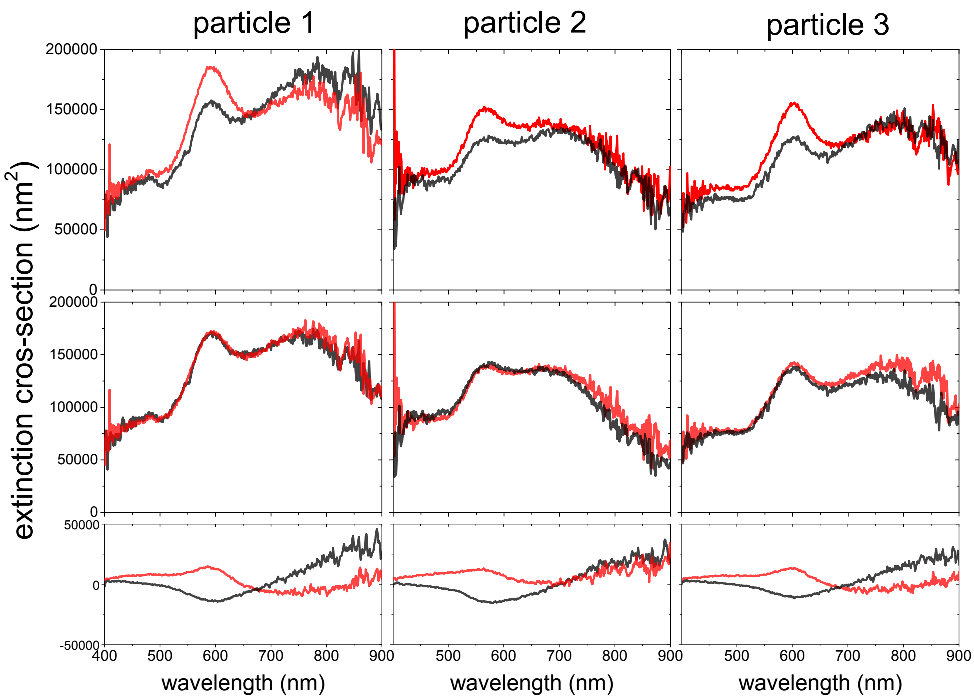

Figure S3: Corrected extinction cross-sections in the backward and forward direction, as well as their sum (total), measured for various 160 nm gold nanocubes supported on a microscope coverslip (red curves: particle in front of the slab (UP position), black curves: particle behind the slab (DOWN position)).

3. Reflection and transmission coefficients at normal incidence (single interface and thin film)

We consider a plane wave (pulsation ω, time-dependence $e^{-i\omega t}$) normally incident on a plane interface between two dielectric media with refractive indexes n_1 and n_2 (Figure S4a). The Fresnel reflection and transmission coefficients are $r_{12} = \frac{n_1 - n_2}{n_1 + n_2}$ and $t_{12} = \frac{2n_1}{n_1 + n_2}$.

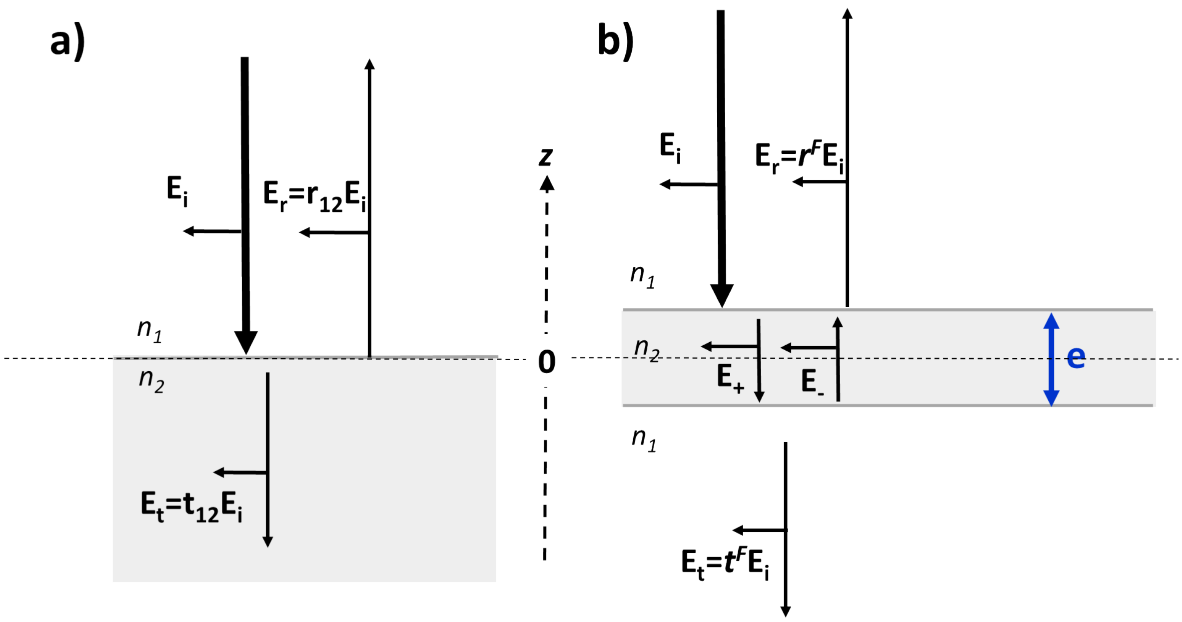

Figure S4: a) Notations for the electric field reflection and transmission of a plane wave at normal incidence on an interface between two dielectric media of refractive indexes n_1 and n_2. b) Case of thin parallel face film of thickness e.

In the case of a thin film with refractive index n_2 and thickness e (Figure S4b), the complex transmission and reflection coefficients write:

$$t^F = \frac{t_{12}t_{21}e^{-i(\Phi_2-\Phi_1)}}{1+r_{12}r_{21}e^{-i2\Phi_2}} \qquad \text{(S1)}$$

and

$$r^F = \left(\frac{r_{12}+r_{21}e^{-i2\Phi_2}}{1+r_{12}r_{21}e^{-i2\Phi_2}}\right)e^{i\Phi_1}$$

, where $k_0 = \frac{\omega}{c}$, $\Phi_1 = en_1k_0$, and $\Phi_2 = en_2k_0$.

These expressions differ from those established p.37 in Ref. [1] in the choice of the origin of the z axis located here at the center of the slab.

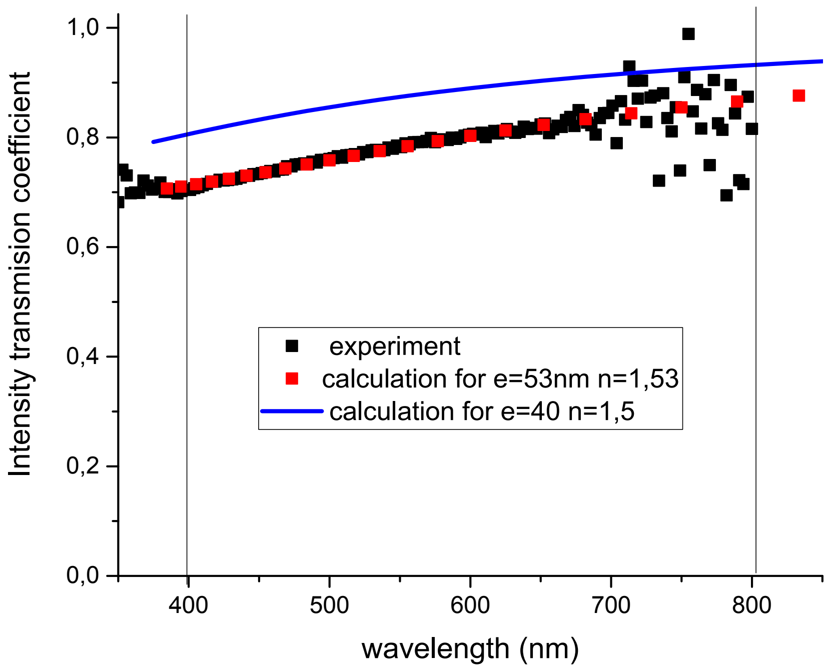

Figure S5: Intensity transmission coefficient measured on a thin Formvar film (black squares) and best fit values (red squares) obtained for e=53 nm and n=1.53 in formula (S1). The blue curve correspond to a thickness e=40nm and a refractive index n=1.5. These last values are chosen throughout the paper for the normalization of measured cross-sections.

4. <u>Calculated extinction cross-sections for a small nanocube supported on a thick substrate</u>

To be closer to the hypotheses made in the approximate model developed in Section 3.2 of the manuscript, extinction cross-sections for reflected and transmitted waves were calculated in the case of a small gold nanocube (20 nm edge) placed at the input or output face of a thick glass slide. They are given in Figure S6 together with the total extinction cross-sections for both configurations.

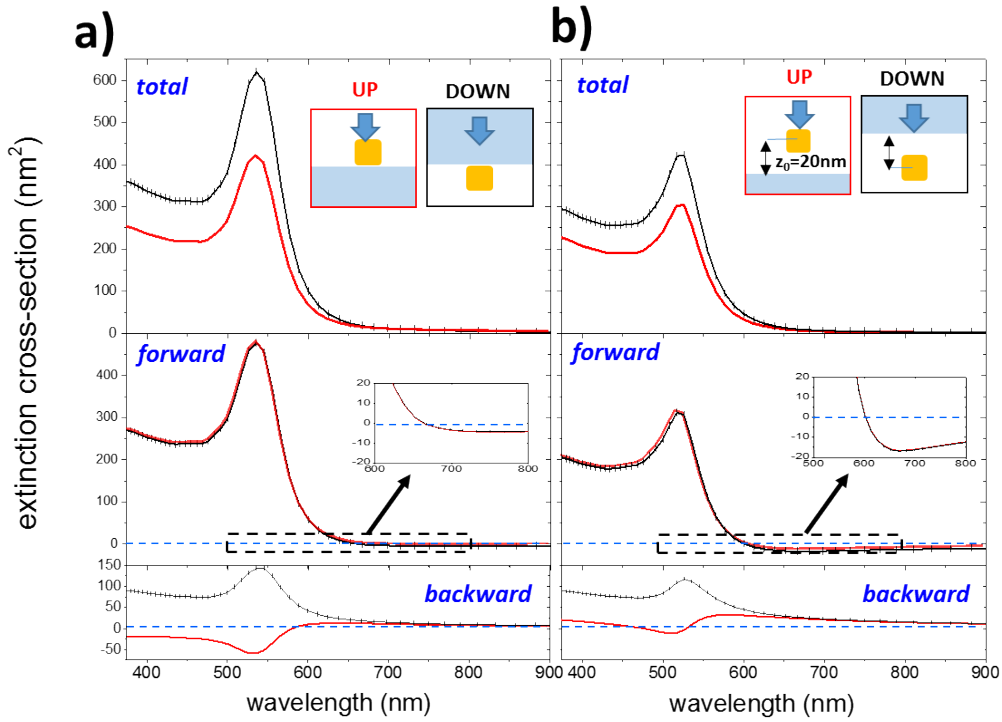

Figure S6: a) Numerical simulations of forward, backward and total extinction cross-sections for a 20 nm gold nanocube in contact with a thick microscope coverslip (interface between air and a dielectric medium of refractive index n=1.5). Red curves: particle placed in front of the substrate, black curves: particle placed behind the substrate. In the forward extinction panel (central), the inset gives a zoomed part of the spectra in the region of sign change. b) The same as a) but for a cube center shifted of 10 nm from the surface.

When the cube is in contact with the substrate (Figure S6a), two observations can be made. First of all, depending on the cube position, the reflected light can either be attenuated or amplified. The cross-sections are almost of opposite sign with similar spectral profiles. This is exactly what can be deduced from relations (9a) and (9b) in the manuscript. Since transmission and reflection coefficients are real, neglecting terms in r^n (with *n*>=2) and assuming $k_0 z_0 << 1$ allows us writing $C_{ext}^{DOWN(r)} \cong r't'tk_0 \operatorname{Im}[\alpha(\omega)]$ and $C_{ext}^{UP(r)} \cong k_0 r \operatorname{Im}[\alpha(\omega)]$. The spectral dependence of $C_{ext}^{DOWN(r)}$ and $C_{ext}^{UP(r)}$ is then simply given by $\operatorname{Im}[\alpha(\omega)]$ which is the one expected for the total extinction (negligible scattering) of a small metallic particle. This is actually in line with the calculations shown in Figure S6a. Moreover, $C_{ext}^{DOWN(r)}$ and $C_{ext}^{UP(r)}$ are in the approximate ratio $\frac{C_{ext}^{DOWN(r)}}{C_{ext}^{UP(r)}} = \frac{r't't}{r} = -t't = -0.96$, $C_{ext}^{DOWN(r)}$ being positively defined (r'>0) which is consistent with numerical simulations, considering that the condition $k_0 z_0 << 1$ is not exactly fulfilled for a 20 nm nanocube.

Secondly, a careful observation of the extinction cross-section for the transmitted light reveals a sign change about 650 nm. This shows that interference effects in relations (7a) and (7b) of the main text can be responsible for an increase of the transmitted power in the forward direction when the total power (reflected + transmitted waves) can only decrease for energy conservation reasons. If the particle is moved away from the interface (see Figure S6b), the relation between extinction cross-sections for the reflected light is less straightforward because the contribution of the phase factors $\mathbf{e}^{\pm i2k_0 z_0}$ becomes more significant. On the other hand, these phase factors induce a much more pronounced change of sign in the extinction cross-section for the transmitted light.

5. Scattering diagrams of a gold nanocube at the air-glass interface

Contrary to the case of the thin film with plane-parallel faces (Figure 8 of the manuscript), the scattered intensity in the forward direction $\left|\mathbf{S}_{scat}(FW)\right|$ is not independent of the particle position at the air-glass interface as illustrated in Figure S7. If we note the scattering Poynting vector expressed from the far-fields scattered in the direction of propagation of the transmitted wave $\mathbf{S}_{scat}(FW)=\frac{1}{2}\mathrm{Re}\left[\widetilde{\mathbf{E}}^{(FW)}\times\widetilde{\mathbf{H}}^{(FW)^*}\right]$ then $\frac{\left|\mathbf{S}_{scat}^{UP}(FW)\right|}{\left|\mathbf{S}_{scat}^{DOWN}(FW)\right|}\neq 1$. The ratio $\frac{\left|\mathbf{S}_{scat}^{UP}(FW)\right|}{\left|\mathbf{S}_{scat}^{DOWN}(FW)\right|}$ can be approximated by the ratio $\frac{S^{UP}(\theta=\pi)}{S^{DOWN}(\theta=0)}$ obtained from the simple model developed in Section 3b of the main text in the case of a small scatterer.

The expressions

$$S^{UP}(\theta=\pi)=\frac{1}{2}\varepsilon_0\, nc\left|\mathbf{E}_\mathbf{S}(\theta=\pi,R)\right|^2$$
$$=\frac{1}{2}n\varepsilon_0\, c\frac{\left|\mathbf{A}^{UP}(\theta=\pi)\right|^2}{R^2}=I_i\, n^3\left|t\right|^2\left(\frac{k_0^2}{4\pi}\right)^2\frac{\left|\alpha(\omega)(1+re^{\mathrm{i}2k_0z_0})\right|^2}{R^2}$$

and

$$S^{DOWN}(\theta=0)=\frac{1}{2}\varepsilon_0\, c\left|\mathbf{E}_\mathbf{S}^{'}(\theta=0,R)\right|^2$$
$$=\frac{1}{2}\varepsilon_0\, c\frac{\left|\mathbf{A}^{DOWN}(\theta=0)\right|^2}{R^2}=I'_i\,\frac{\left|t'\right|^2}{n}\left(\frac{k_0^2}{4\pi}\right)^2\frac{\left|\alpha(\omega)(1+re^{\mathrm{i}2k_0z_0})\right|^2}{R^2}$$

give $\dfrac{S^{UP}(\theta=\pi)}{S^{DOWN}(\theta=0)}=\dfrac{n^4t^2}{t'^2}=n^2=2.25$ (for n=1.5 and identical intensities of the exciting waves assumed in both configurations $\dfrac{I'_i}{I_i}=1$) . This value is of the order but less than the value that can be graphically estimated in Figure S7 from numerical calculations with a 160 nm gold nanocube. The difference can be explained by fact that the NP size is large and deviates from the condition required for the applicability of the model developed in Section 3.2.

In any case, the ratio $\dfrac{S^{UP}(\theta=\pi)}{S^{DOWN}(\theta=0)}$ deviates from the unity contrary to the case of the thin film (Figure 8 of the main text). Actually, for a single interface, the transmitted wave does not propagate in air in both configurations but either in air (DOWN position) or inside the dielectric (UP position) with regard to Fig.S7.

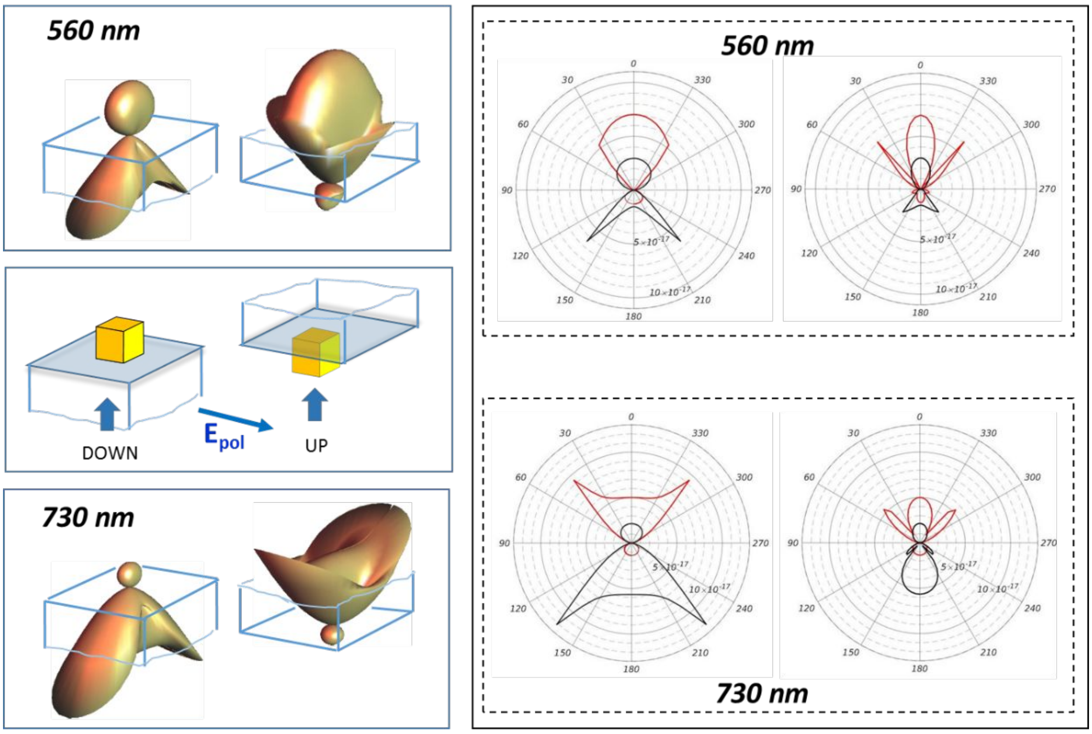

Figure S7: Left: 3D free space radiation patterns (scattering Poynting vector amplitude as a function of the scattering direction) of a cube placed in a UP or DOWN position relative to the thick substrate. The incident light is linearly polarized along the direction specified. Diagrams are given for two wavelengths (560 nm and 730 nm) close to the plasmon resonances of quadrupolar and dipolar character (see Figure 6 of the main text). The intensities of the incident waves are chosen equal for both configurations. Right: 2D patterns projected in the planes parallel and perpendicular to the direction of polarization. The red curves correspond to the UP position and the black curves to the DOWN position. The 0° polar angle (vertical direction in upper half-circle) corresponds to the direction of the transmitted wave.

A way to unify the descriptions of the thin film and the thick glass slide would be to apply the optical theorem not inside the dielectric medium just after the transmission through the first interface but in the air, after the transmission through the **second** interface as already discussed in Section 3.2. For illustration, we first consider the case where the particle is placed above the substrate relative to the incident beam direction (UP position). It is first necessary to construct the far-field $\hat{\mathbf{E}}_S$ scattered in the upperr-half space **after** its refraction through the dielectric-air interface. One can use relation (6b) of the manuscript to determine a new vector amplitude of this field $\hat{\mathbf{A}}_{air}^{UP}(\theta=\pi)$, noting that the refractive index of the output medium is now n=1 and the transmission coefficient of the whole slab is the product tt', $\mathbf{E'}_t = tt'\mathbf{E}_i$ being the field transmitted in air after a direct crossing of both the air-dielectric and dielectric air interfaces.

We get from (6b)

$$\hat{\mathbf{A}}_{air}^{UP}(\theta=\pi)=\frac{k_0^2}{4\pi\varepsilon_0}\mu^{UP}\ n(=1)\,t\,(=tt')e^{\mathrm{i}k_0z_0}\mathbf{e}_x$$
$$=\frac{k_0^2}{4\pi}\alpha(\omega)(tt')E_i\ (e^{-\mathrm{i}k_0z_0}+re^{\mathrm{i}k_0z_0})\ e^{\mathrm{i}k_0z_0}\mathbf{e}_x$$

with $\boldsymbol{\mu}^{UP}=\varepsilon_0\alpha(\omega)(\mathbf{E}_ie^{-\mathrm{i}k_0z_0}+\mathbf{E}_re^{\mathrm{i}k_0z_0})=\varepsilon_0\alpha(\omega)\mathbf{E}_i(e^{-\mathrm{i}k_0z_0}+re^{\mathrm{i}k_0z_0})$ given in the main text.

The corresponding scattering intensity in the forward direction $(\theta=\pi)$ is now

$$\hat{S}^{UP}(\theta=\pi)=\frac{1}{2}\varepsilon_0\,c\left|\hat{\mathbf{E}}_S(\theta=\pi,R)\right|^2$$
$$=\frac{1}{2}\varepsilon_0\,c\frac{\left|\hat{\mathbf{A}}_{air}^{UP}(\theta=\pi)\right|^2}{R^2}$$

Concerning the case where the particle is in a DOWN position, $\hat{S}^{DOWN}(\theta=0)$ is unchanged.

$$\hat{S}^{DOWN}(\theta=0)=\frac{1}{2}\varepsilon_0\,c\left|\hat{\mathbf{E}}_S(\theta=0,R)\right|^2$$
$$=\frac{1}{2}\varepsilon_0\,c\frac{\left|\hat{\mathbf{A}}^{DOWN}(\theta=0)\right|^2}{R^2}$$

, with $\hat{\mathbf{A}}^{DOWN}(\theta=0)=\dfrac{k_0^2}{4\pi\varepsilon_0}\mu^{DOWN}\ (e^{-\mathrm{i}k_0z_0}+re^{\mathrm{i}k_0z_0})\mathbf{e}_x=\dfrac{k_0^2}{4\pi}\alpha(\omega)tt'E_i(e^{-\mathrm{i}k_0z_0}+re^{\mathrm{i}k_0z_0})e^{\mathrm{i}k_0z_0}\mathbf{e}_x$

from (6b) and $\boldsymbol{\mu}^{DOWN}=\varepsilon_0\alpha(\omega)\mathbf{E}'_t\,e^{\mathrm{i}k_0z_0}=\varepsilon_0\alpha(\omega)tt'\mathbf{E}_ie^{\mathrm{i}k_0z_0}$ as given in the main text.

The vector amplitudes $\hat{\mathbf{A}}^{DOWN}(\theta=0)$ and $\hat{\mathbf{A}}^{UP}(\theta=\pi)$ are now identical and we obtain a ratio $\dfrac{\hat{S}_{air}^{UP}(\theta=\pi)}{\hat{S}^{DOWN}(\theta=0)}$=1, just as for the thin film.

The application of the GOT also allows us to show that the extinguished transmitted powers calculated in this framework are the same for a UP and a DOWN position of the polarizable dipole

$$\hat{P}_{ext}^{UP(t)}=\frac{2\pi\ \varepsilon_0\ c}{k_0}\mathrm{Im}\left[\mathbf{E}'^*_t.\hat{\mathbf{A}}_{air}^{UP}(\theta=\pi)\right]=\hat{P}_{ext}^{DOWN(t)}=\frac{2\pi\ \varepsilon_0\ c}{k_0}\mathrm{Im}\left[\mathbf{E}'^*_t.\hat{\mathbf{A}}_{air}^{DOWN}(\theta=\pi)\right]$$
$$=\frac{2\pi\ \varepsilon_0\ c}{k_0}\frac{k_0^2}{4\pi}(tt')^2\ \mathrm{Im}\left[(tt')^2E_i^*\varepsilon_0\alpha(\omega)E_i\ (e^{-\mathrm{i}k_0z_0}+re^{\mathrm{i}k_0z_0})\ e^{\mathrm{i}k_0z_0}\right]$$
$$=I_ik_0\,(tt')^2\ \mathrm{Im}\left[\alpha(\omega)(1+re^{\mathrm{i}2k_0z_0})\ \right]$$

These powers are those that are expected to be measured in our experimental configuration ($\Delta P_{UP}^{FW}$and ΔP_{DOWN}^{FW}) and that give the equal extinction cross-sections $\mathfrak{C}_{ext}^{FW(UP)}=\frac{\Delta P_{UP}^{FW}}{I'_t}=k_0Im\left[\alpha(\omega)(1+re^{i2k_0z_0}\right]$ and $\mathfrak{C}_{ext}^{FW(DOWN)}=\frac{\Delta P_{DOWN}^{FW}}{I'_t}=k_0Im\left[\alpha(\omega)(1+re^{i2k_0z_0}\right]$.

These cross-sections differ from $C_{ext}^{UP(t)}$ and $C_{ext}^{DOWN(t)}$ defined in (7a) and (7b) of the manuscript by a common factor $nt^2=\dfrac{t'^2}{n}$ for a normal incidence. We recognize here the factor Θ established in Section 3.3 of the manuscript.

<u>REFERENCES</u>

(1) Bohren, C. F.; Huffman, D. P., *Absorption and Scattering of Light by Small Particles*. Wiley: New York, 1983.

(2) Novotny, L.; Hecht, B., *Principles of Nano-Optics*. Cambridge University Press: New York, 2006.